Constitutive model and analysis of creep flow of natural slopes

O. Cazacu*, Nicolae D. Cristescu*

Summary

A new model for describing creeping of natural slopes is proposed. The geological material in the slope is modeled with a non-homogeneous Bingham constitutive equation [Cristescu *et al.*, 1998]. This constitutive equation accounts for the effect of gravitational compaction on the material response and allows for a variation of density and yield stress with depth. A criterion for shear flow initiation is formulated and the ensuing motion is described. A straightforward procedure for determination of the parameters of the model based only on field data is presented. To illustrate this procedure and the suitability and potential of the proposed approach, field data reported in the literature have been used to predict the behaviour (measured displacements distribution) of landslides from two sites (in Switzerland and in Italy). Comparison between the theoretical predictions and measured displacement profiles are reasonably good, with accuracy within the experimental scatter.

1. Introduction

Many natural slopes exhibit slow movements due to the viscous response of the geologic material in the slope, to changes in geometry, static and hydraulic boundary conditions, and sometimes to chemical environment. Although long-term sliding velocities can be of the order of centimeters per year [Brunsden, 1984; Vulliet and Hutter, 1988b; D'Elia *et al.*, 1998; etc.], short term fluctuations may be ten times larger or more and on occasion can cause catastrophic landslides resulting in damage of structures (e.g. roads, buildings) and loss of human life. Due to the importance of evaluation of landslide risk, in the last decades great efforts have been devoted to analyzing, modelling, and predicting such phenomena. Conventional stability analyses, which treat the geologic material in the slope as a rigid perfectly plastic body, may provide information on the safety factor of stable mass of soil but cannot simulate the kinematics (displacements profiles, velocity fields) of those continuous creeping natural slopes. To describe gravitational creep flow, a variety of rate-dependent constitutive equations have been used. The soil was treated either as a non-Newtonian viscous fluid [*e.g.* Vulliet and Hutter, 1988a; Angey *et al.*, 1996; etc.], Bingham fluid [*e.g.* Liu and Mei, 1989], Bingham fluid with viscosity that varies linearly with time [*e.g.* Ter-Stepanian, 1973], Bingham fluid with 2 viscosity coefficients [*e.g.* Sousa and Voight, 1991] or as a mixture of an inviscid interstitial fluid and non-Newtonian viscous fluid matrix [*e.g.* Vulliet and Hutter, 1988b; Hutter, 1993]. Based on field observations (inclinometer measurements taken from Swiss and French landslides), [Vulliet, 1988c], proposed a 3D viscous model that can describe the slow motion of natural slopes which may deform within their body and slide along their basal surface. It is considered that strong localized shear deformation occurs in a thin layer close to the base, the deformation being treated as a finite jump in velocity on the basal surface. The model simulates well shallow landslides in progress but does not account for the initiation (starting phase) of the movement. A model aimed at describing the flow of an initially stationary mass of cohesionless granular material down rough curved beds was proposed by Savage and Hutter [1991]. The constitutive assumptions are rather restrictive: the material in the slope is treated as an incompressible Mohr-Coulomb type continuum and the basal friction law is a rate-independent Coulomb-type friction law. Among more recent studies, which are more related to the approach adopted in the present paper, let us mention the work of Desai and coworkers [see for example, Desai *et al.*, 1995; Samtani *et al.*, 1996]. The theory of elastoviscoplasticity of [Perzyna, 1966] is used together with the hierarchical single-surface plasticity model of Desai to describe the soil and the basal surfaces involved in creeping slopes. The model was calibrated from a series of laboratory tests on samples obtained from the field site of Villarbeney, Switzerland and was implemented in a 2D finite-element procedure [see Samtani *et al.*, 1996]. Based on the analysis of the compaction due to self-weight of an elastic/viscoplastic material deposited on an inclined plane, [Cristescu *et al.*, 1998] have proposed

* Department of Aerospace Engineering, Mechanics & Engineering Science, University of Florida, Gainesville.

a new non-homogeneous Bingham model with density dependent yield stress. The model was further applied to the study of flow initiation and ensuing motion of a granular material down a chute for different slip conditions at the interface and for several rate-dependent viscous sliding laws.

In the present paper the non-homogeneous Bingham model [CRISTESCU *et al.*, 1998; CRISTESCU *et al.*, 2000] is applied to the analysis and prediction of landslides in which the creep deformations within the landslide body are significant. The case of mudslides, which advance by sliding on a discrete boundary slip surface, so the contribution of creep deformation within the mudslide are generally small in comparison to the displacements cumulated along the slip surface, is not considered in the present paper. The model presented in this paper describes the main features of the observed behavior of most creeping natural slopes such as the existence of a shear zone involving severe translational displacements and the depth at which shear flow initiates, the existence of a stationary zone below the shear zone, and a rigid body like motion above the shear zone (plug flow). The extent of the shear zone and the variation of its thickness in relation to changes in the density and yield limit at the ground surface also result from the theory. A straightforward procedure for determination of the parameters involved in the law of variation of the yield stress with depth based solely on field data is presented. Finally, the model proposed is used to describe the movements of two natural slopes (a) Villarbeney, Switzerland [data reported in DESAI *et al.*, 1995] and (b) Fosso San Martino, Italy [data after BERTINI *et al.*, 1984]. Comparison between the theoretical predictions and measured displacement profiles are reasonably good, with accuracy within the experimental scatter.

2. Constitutive model and analysis of creeping slopes

To describe the slow and continuous movement of natural slopes under gravity, we consider that the geologic material obeys a non-homogeneous Bingham model [see CRISTESCU *et al.*, 1998] of the form

$$D=\begin{cases} 0 \;\; if \;\; II_{T'} \le k^2(\rho) \\ \dfrac{1}{2\eta(\rho)}\left\langle 1-\dfrac{k(\rho)}{\sqrt{II_{T'}}}\right\rangle T' \;\; if \;\; II_{T'} > k^2(\rho) \end{cases} \qquad (1)$$

where D is the stretching tensor, $D_{ij}=\frac{1}{2}(v_{i,j}+v_{j,i})$, v the velocity field, $T'=T-\frac{1}{3}(tr\,T)\,I$, the stress deviator (tr (.) is the trace operator), while $II_{T'}=\frac{1}{2}\,T'_{ij}\,T'_{ij}$ is the second invariant of $\boldsymbol{T}'$; $k(\rho)$ is the yield stress which is assumed to be a function of the current density ρ, and $\eta(\rho)$ is a density dependent viscosity. The geometry of the natural slope and the related coordinate system is shown in Fig. 1: θ is the slope angle, the x-axis along the slope direction, y-axis normal to the x-axis and situated in the slope plane. We make the usual kinematic assumption that the particles move in the slope direction with a velocity depending on depth only, *i.e*:

$$v_x=V(y)\,, \quad v_y=0\,, \quad v_z=0 \qquad (2)$$

so that the stretching tensor $\boldsymbol{D}$ is

$$D=\frac{\partial V}{\partial y}\begin{bmatrix} 0 & 1 & 0 \\ 1 & 0 & 0 \\ 0 & 0 & 0 \end{bmatrix} \qquad (3)$$

Most data support a linear dependence of the unit weight of soil with depth.(*e.g.* [DESAI *et al.*, 1995] *i.e.*

$$\gamma(y)=\gamma_0+\alpha y/\cos\theta \qquad (4)$$

where $\gamma=\rho g$ is the unit weight at the depth $y\cos\theta$, γ_0 is the unit weight at the surface.

Note that the continuity equation reduces to $\partial\rho/\partial t = 0$, since from the kinematic assumption (2) the only non-zero velocity component is the x-component and the density is a function of y, only (see Eq. 4).

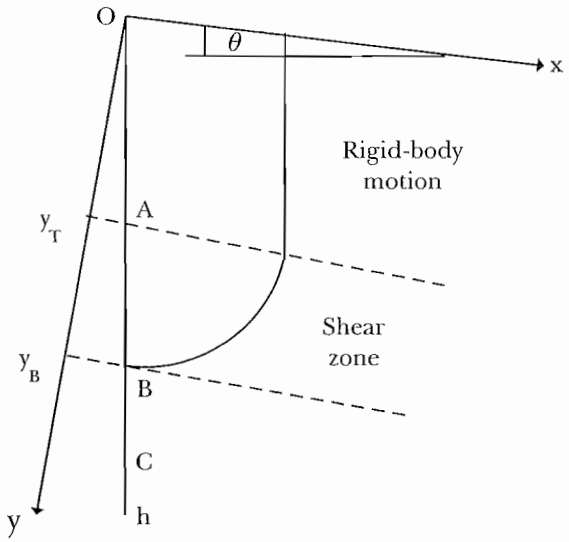

Fig. 1 – Schematic diagram of the flow of a creeping slope and notations used.

Fig. 1 – Diagramma schematico del flusso lento di un pendio e notazione utilizzata.

Substituting (3) in the constitutive law (1) we obtain (stresses are negative in compression):

$$T_{xx}=T_{yy}=T_{zz}=\sigma \quad and \quad T_{xz}=T_{yz}=0 \tag{5}$$

where $\sigma = tr(\mathbf{T})/3$ is the mean stress. Next, balance of linear momentum together with (5) yield

$$\begin{aligned}&\frac{\partial\sigma}{\partial x}+\frac{\partial T_{xy}}{\partial y}+\gamma\sin\theta=0\\&\frac{\partial\sigma}{\partial y}+\frac{\partial T_{xy}}{\partial x}+\gamma\cos\theta=0\\&\frac{\partial\sigma}{\partial z}=0.\end{aligned} \tag{6}$$

Assuming that the *yield limit depends solely on depth*, it follows that the shear stress T_{xy} is a function of y, hence

$$T_{xy}=-\sin\theta\int_0^y\gamma(y)\,dy+T_0 \tag{7}$$

and the mean stress is

$$\sigma=\sigma(y)=-\cos\theta\int_0^y\gamma(y)\,dy+\sigma_0 \tag{8}$$

where σ_0 and T_0 are the mean stress and shear stress at the ground surface, respectively. In most cases, σ_0 and T_0 can be considered to be zero. For the specific law of linear variation of γ with depth (4), we obtain

$$\begin{aligned}&T_{xy}(y)=-\left(\frac{\alpha}{2}\tan\theta\right)y^2-\gamma_0\sin\theta\,y+T_0,\\&\sigma(y)=-\frac{\alpha}{2}y^2-\gamma_0\cos\theta\,y+\sigma_0\end{aligned} \tag{9}$$

The shear stress and the mean stress are increasing function of *depth*.

In the model the yield stress is a function of the actual density [see Eq. (1)]. Since the density varies with depth, we further assume that the yield stress is a function of depth only. Thus, the model exhibits tranverse isotropy, *i.e.* the material is isotropic in any plane y =constant (the group of symmetry of the material consists of all the rotations about the y direction).

While most data support a linear variation of density with depth [see Eq. (4)], a linear variation of the yield stress with depth is physically unacceptable [for a rigorous proof of this statement see CRISTESCU *et al.*, 2000]. For sake of simplicity, we postulate a power law variation of the yield stress with depth,

$$k(y)=k_0+\beta\left(\frac{y}{y_0}\right)^n \tag{10}$$

where $k_0 = k(0)$ is the yield stress at the ground surface, n and β are material constants, y_0 is a reference depth.

According to the constitutive law (2), flow takes place if and only if $|T_{xy}(y)| > k(y)$ *i.e.*, when the shear stress surpasses the yield limit. The threshold condition for *flow initiation* is therefore $|T_{xy}(y)| > k(y)$. As an illustration of the capabilities of the model in the following we describe the theoretical pattern of movements corresponding to $n = 2$ in the power law (10). A general procedure for determination of n and β from field data will be presented in the next section. Let us denote by h the overall depth of the slope (see Fig. 1), $\gamma_h = \gamma(h)$ the unit weight at the depth h and $k_h = k(h)$ the corresponding yield limit. The expressions of the phenomenological coefficient α in terms of the unit weights at the ground surface and at the depth h, and of β in terms of the yield limits at the same levels, are

$$\begin{aligned}&\alpha=\frac{\gamma_h-\gamma_0}{h}\\&\frac{\beta}{y_0^2}=\frac{k_h-k_0}{h^2\cos^2\theta}\end{aligned} \tag{11}$$

Hence, the condition for flow initiation $|T_{xy}(y)| > k(y)$ writes:

$$\left(\frac{\gamma_h-\gamma_0}{2h}\tan\theta-\frac{k_h-k_0}{h^2\cos^2\theta}\right)y^2+(\gamma_0\sin\theta)\,y+|T_0|-k_0=0 \tag{12}$$

The case $\frac{\gamma_h-\gamma_0}{2h}\tan\theta-\frac{k_h-k_0}{h^2\cos^2\theta}=0$ corresponding to an overall depth of the moving slope given by $h=\frac{2(k_h-k_0)}{(\gamma_h-\gamma_0)\sin\theta\cos\theta}$ is physically unacceptable and will not be considered.

For $h<\frac{2(k_h-k_0)}{(\gamma_h-\gamma_0)\sin\theta\cos\theta}$, the discriminant of (12) considered as a second order polynomial in $y/\cos\theta$ is

$$\Delta=\frac{1}{h^2}\left[h^2\gamma_0^2\sin^2\theta\cos^2\theta+2k_0h(\gamma_h-\gamma_0)\cdot\sin\theta\cos\theta+4(k_0-|T_0|)(k_0-k_h)\right].$$

For θ fixed, the discriminant of $\Delta(h)=0$, as second order polynomial in h is

$$\Delta_1=4\left[k_0^2(\gamma_h-\gamma_0)^2+4(k_0-|T_0|)(k_h-k_0)\gamma_0^2\right] \tag{13}$$

Since $k_h \geq k_0$, $k_0 \geq |T_0|$, $\Delta(h) =$ has a unique positive root h^*, where

$$h^*=\frac{-k_0(\gamma_h-\gamma_0)+\sqrt{k_0^2(\gamma_h-\gamma_0)^2+4(k_0-|T_0|)(k_h-k_0)\gamma_0^2}}{\gamma_0^2\sin\theta\cos\theta} \tag{14}$$

In conclusion,

- If $h = h^*$, incipient shearing motion initiates at the depth

$$h_{Yi}=\frac{\gamma_0\sin\theta\cos\theta}{2\left[\frac{k_h-k_0}{h_*^2}-\frac{\gamma_h-\gamma_0}{2h^*}\sin\theta\cos\theta\right]} \tag{15}$$

and $T_{xy}(y)<k(y)$ for any $y \neq h_{Yi}\cos\theta$; the top stratum $0 \le y \le h_{Yi}\cos\theta$ is a rigid plug in motion, while the bottom stratum $h_{Yi}\cos\theta \le y \le h^*\cos\theta$ is at rest.

- If $h > h^*$, $\Delta > 0$ so (11) has two distinct solutions: y_B corresponding to the lower level of the shear zone, and y_T corresponding to the top of the shear zone. In this case, $|T_{xy}(y)| > k(y)$ for $y_b < y < y_T$ and $|T_{xy}(y)| < k(y)$ otherwise. The pattern of movement of the creeping slope is as depicted in Fig. 1. There is a shear zone $y_T < y < y_B$, its lower and upper boundaries being the solutions of equation (12), *i.e.*:

$$y_T=\frac{-\gamma_0 h\sin\theta\cos\theta}{2\left[\frac{\gamma_h-\gamma_0}{2}\sin\theta-\frac{k_h-k_0}{h\cos\theta}\right]}+$$

$$+\frac{\sqrt{h^2\gamma_0^2\sin^2\theta\cos^2\theta+2k_0h(\gamma_h-\gamma_0)\sin\theta\cos\theta+4(k_0-|T_0|)(k_0-k_h)}}{2\left[\frac{\gamma_h-\gamma_0}{2}\sin\theta-\frac{k_h-k_0}{h\cos\theta}\right]}$$

$$y_B=\frac{-\gamma_0 h\sin\theta\cos\theta}{2\left[\frac{\gamma_h-\gamma_0}{2}\sin\theta-\frac{k_h-k_0}{h\cos\theta}\right]}-$$

$$-\frac{\sqrt{h^2\gamma_0^2\sin^2\theta\cos^2\theta+2k_0h(\gamma_h-\gamma_0)\sin\theta\cos\theta+4(k_0-|T_0|)(k_0-k_h)}}{2\left[\frac{\gamma_h-\gamma_0}{2}\sin\theta-\frac{k_h-k_0}{h\cos\theta}\right]} \tag{16}$$

the upper stratum $0 < y < y_T$ moves as a rigid, while the bottom mass is stationary. In general, the extent of the shear zone strongly depends on the magnitude of the yield stress k_h. If k_h is very small, the thickness of the moving stratum becomes very small (i.e., if $k_h \to 0$ it follows $y_T \to 0$). As an example, in Fig.2a is shown the variation of the shear stress $T_{xy}(y)$ and of the yield limit $k(y)$ with depth corresponding to $\theta = 20°$,

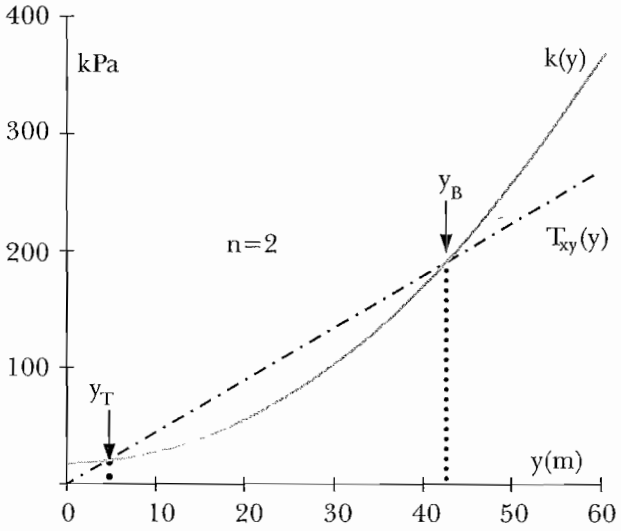

Fig. 2a - Variation of the shear stress $T_{xy}(y)$ and of the yield limit $k(y)$ for $n = 2$; in the layer $y_T < y < y_B$ $|Txy(y)| > k(y)$ so the material is shearing, while for $y < y_T$ the material is in plug rigid motion.

Fig. 2a – Variazione dello sforzo di taglio $T_{xy}(y)$ e della tensione di plasticizzazione $k(y)$ per $n = 2$; nello strato $y_T < y < y_B$ $|Txy(y)| > k(y)$ per cui il materiale subisce scorrimenti, mentre per $y < y_T$ il terreno è in moto rigido.

$k_0 = 12$ kPa, $\beta = 0.1$ kPa, $T_0 = 0$ kPa, $\gamma_0 = 12$ kN/m^3, $\alpha = 0.05$ kN/m^4. For this set of values of the constitutive parameters the limits of the shear zone are $y_T = 3.72$ m and $y_B = 41.4$ m. Note that from (12) it also follows that there is an inclination $\theta = \theta_C$ such that the overall depth of the moving slope is h *i.e.* $T_{xy}(h\cos\theta_C) = k_h$

$$\sin 2\theta_c=\frac{2k_h}{\frac{\gamma_h+\gamma_0}{2}h}. \tag{17}$$

In this case, the lower boundary of the shear zone is $y_B = h\cos\theta$, while the upper boundary is

$$y_T=y_B\frac{(k_0-|T_0|)}{2k_h\gamma_0-k_0(\gamma_0+\gamma_h)}.$$

Velocity distribution in the shear zone

In the shear zone

$$2\eta(y)D_{xy}=T_{xy}-k(y)(sign\,T_{xy}) \tag{18}$$

and since from (9) we have $sign T_{xy} = -1$, we get

$$D_{xy}=\frac{-1}{2\eta(y)}\left[|T_{xy}(y)|-k(y)\right] \quad for \quad y_T<y<y_B$$
$$D_{xy}=0 \quad for \quad 0\le y\le y_T \quad and \quad y_B\le y\le h\cos\theta \tag{19}$$

$|T_{xy}(y)| - k(y)$ being the "overstress" which is a function of depth. Assuming $T_0 = 0$ and substituting (3), (8), (10) in (19) we obtain

$$\frac{dV}{dy}=\frac{-1}{\eta}\left\langle\left[\frac{\gamma_h-\gamma_0}{2h}\tan\theta y^2+\gamma_0\sin\theta y\right]-\frac{k_h-k_0}{h^n}\left(\frac{y}{h\cos\theta}\right)^n-k_h\right\rangle \tag{20}$$

For sake of simplicity, we assume that the viscosity η is constant. If there is no slip at the bottom, i.e., for $V(y_B) = 0$, by integrating (20) we get the velocity distribution in the shear zone $y_T < y < y_B$:

$$V(y)=\frac{(y_B-y)}{\eta}\left[\frac{\gamma_h-\gamma_0}{6}(y_B^2+y^2+y\cdot y_B)+\frac{\gamma_0\sin\theta}{2}(y_B+y)-k_0\right] \tag{21}$$

The top layer $0 < y < y_T$ moves as a rigid with the velocity $V(y_T)$ of the layer $y = y_T$.

As an example in Fig.2b is shown the computed displacement profile after $\Delta t = 100$ days for $\theta = 20°$, $n = 2$, $k_0 = 12$ kPa, $\beta = 0.1$ kPa, $T_0 = 0$ kPa, $\gamma_0 = 12$ kN/m^3, $\alpha = 0.05$ kN/m^4, $\eta = 1.4 \times 10^5$ Poise. Generally, even after flow has initiated the material will further compact if the stress to which it is subjected is below the compressibility/dilatancy boundary of the material (for this concept see [CRISTESCU, 1989]. Compaction results in an increase of the yield limit, which causes a decrease in the displacement rate to extremely low values. Conversely, a decrease in yield stress and an increase in the unit weight of the soil may be caused for instance by heavy rainfalls or sudden snow melting. This in turn, results in a higher displacement rate. Fig. 3 demonstrates this point. Setting $\theta = 20°$, $n = 2$, $k_0 = 12$ kPa, $\beta = 0.1$ kPa, $T_0 = 0$ kPa, $\alpha = 0.05$ kN/m^4, for higher γ_0 and lower yield limits k_0 we obtain a larger shear deformation zone, a thinner rigid layer, and more severe displacements. The three displacement profiles shown correspond to ($k_0 = 14$ kN, γ_0=12 kN/m^3), ($k_0 = 13$ kN, γ_0 =12.4 kN/m^3), and ($k_0 = 11.5$ kN, γ_0 =13 kN/m^3), respectively. Sudden rate increase may also be the consequence of debris accumulation [see D'ELIA *et al.*, 1998] which determines an increase of the shear stress at the ground surface. Fig.4 show the influence of T_0 when all the other parameters are fixed ($\theta = 20°$, $n = 2$, $k_0 = 12$ kPa, $\gamma_0 = 12$ kN/m^3, $\beta = 0.1$ kPa, $T_0 = 0$ kPa, $\alpha = 0.05$ kN/m^4). If $|T_0|$ increases from 0 to 10 kPa the shear deformation zone extends up to the ground surface ($y_{|T0|=10} = 0.01$m) and the relative displacements are larger (see Fig. 4).

In the examples presented above we have assumed that the viscosity η is constant, because from the available data the determination of the variation of viscosity with depth or humidity was not possible.

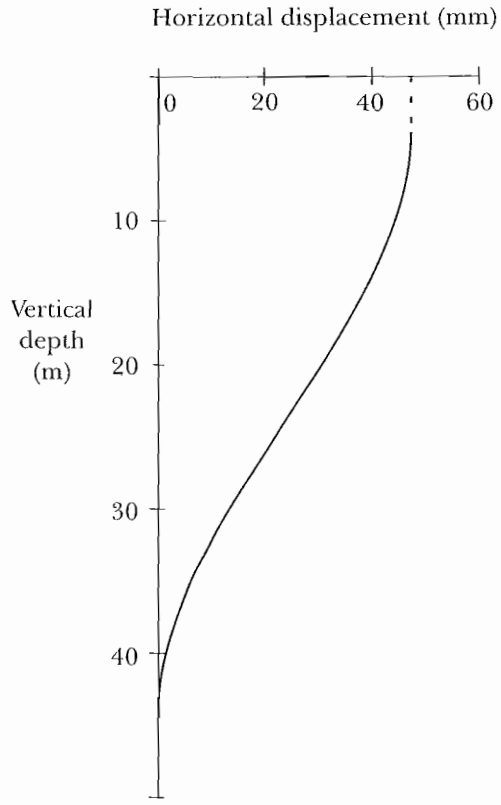

Fig. 2b - Displacement profile obtained after 100 days ($\eta = 1.4 \times 10^5$ Poise); the dotted line marks the plug flow.
Fig. 2b - Andamento degli spostamenti calcolati dopo 100 giorni ($\eta = 1.4 \times 10^5$ Poise); la linea tratteggiata indica il livello del moto rigido.

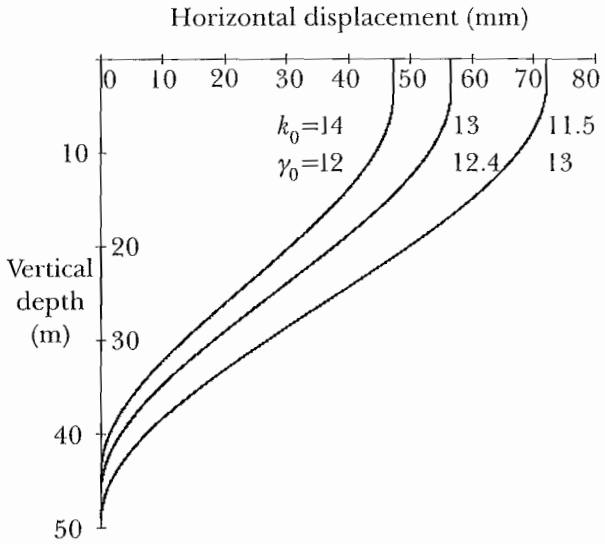

Fig. 3 – Influence of the unit weight and yield limit at the ground surface on the displacement rate and the extent of the shear zone and rigid motion zone, respectively.
Fig. 3 - Influenza del peso specifico e della tensione di plasticizzazione alla superficie libera del terreno sulla velocità di spostamento e dell'ampiezza della zona di scorrimento e della zona con moto rigido.

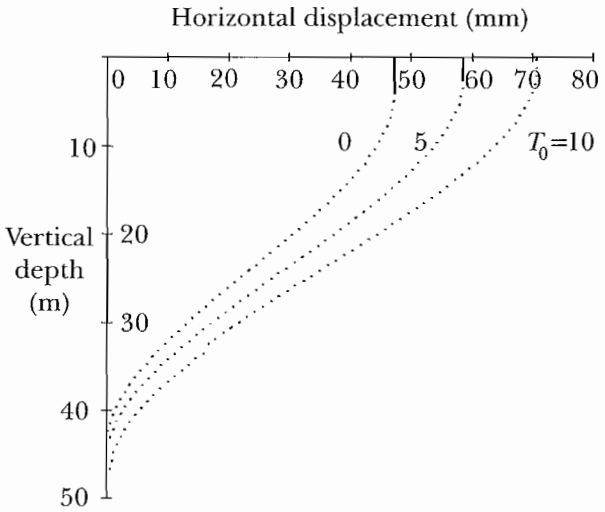

Fig. 4 – Influence of the ground surface shear stress T_0 on displacement rate showing that large values of T_0 may reduce the top rigid motion layer to zero.
Fig. 4 – Influenza della tensione di taglio T_0 alla superficie sulla velocità di spostamento; si mostra che alti valori di T_0 possono ridurre a zero l'ampiezza dello strato superficiale in moto rigido.

3. Procedure for determination of the constitutive parameters from field measurements

Laboratory experiments are far from being representative of long-term *in situ* behaviours. On the other hand, movements of natural slopes are difficult to measure and the instrumentation is complex. Our approach is to use a minimum of commonly recorded data, such as inclinometer readings to estimate the constitutive parameters involved in the proposed model. Most creeping slopes exhibit deformation profiles similar to those given in Fig. 1. *i.e.* there is an upper layer OA in rigid motion, zone AB experiences relative shear displacements, while zone BC can be considered stationary. Since $|T_{xy}(y_T)| = k(y_T)$ and $|T_{xy}(y_B)| = k(y_B)$, the coefficients n and β involved the law of variation of the yield limit with depth (see (10)) can be estimated based on the measured values y_T and y_B of the upper and lower limits of the shear zone, and the yield limit k_0, as:

$$n = \frac{\ln\left(\frac{\left(\frac{\alpha}{2}\tan\theta\right)y_B^2 - \gamma_0 y_B \sin\theta + |T_0| - k_0}{\left(\frac{\alpha}{2}\tan\theta\right)y_T^2 - \gamma_0 y_T \sin\theta + |T_0| - k_0}\right)}{\ln\left(\frac{y_B}{y_T}\right)}$$

$$\beta = \frac{\gamma_0 \sin\theta (y_B - y_T) + \frac{\alpha}{2}(y_B - y_T)^2 \tan\theta}{\left(\frac{y_T}{y_0}\right)^n - \left(\frac{y_B}{y_0}\right)^n}, \qquad (22)$$

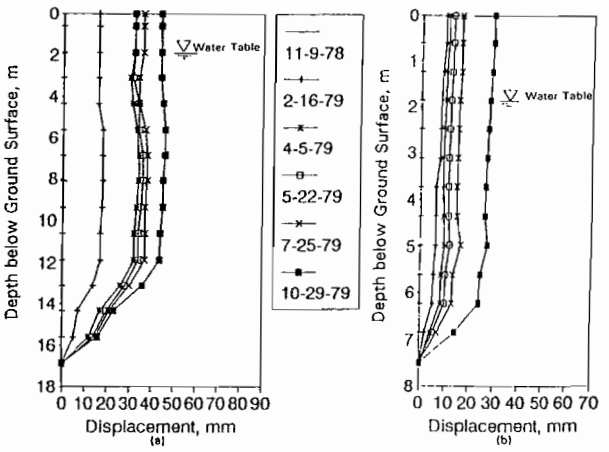

Fig. 5 – Observed inclinometer profiles at boreholes: (a) E_1; and (b) E_2 [after DESAI *et al.*, 1995].
Fig. 5 – Profili di spostamento degli inclinometri: (a) E_1; e (b) E_2 [da Desai et al., *1995].*

The values retained for the parameters k_0, γ_0, and α will correspond to the mean values of the cohesion and unit weight of the material at the ground surface at the given location. Further, inclinometers readings after a given time interval Δt permit the calibration of the viscosity coefficient η. Indeed, assuming $V(y_B) = 0$ and using (21), we obtain

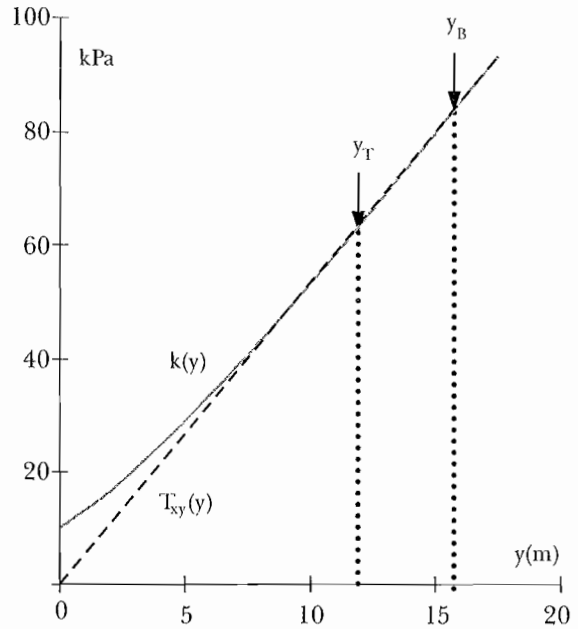

Fig. 6 – Theoretical variation of the shear stress and yield limit with depth for Villaberney landslide, location E_1; for $y_T < y < y_B$: $|T_{xy}(y)| > k(y)$ and creep flow takes place
Fig. 6 – Variazione teorica con la profondità della tensione tangenziale e della tensione di plasticizzazione per la frana di Villaberney, E_1; per $y_T < y < y_B$: $|T_{xy}(y)| > k(y)$ e quindi si ha scorrimento lento.

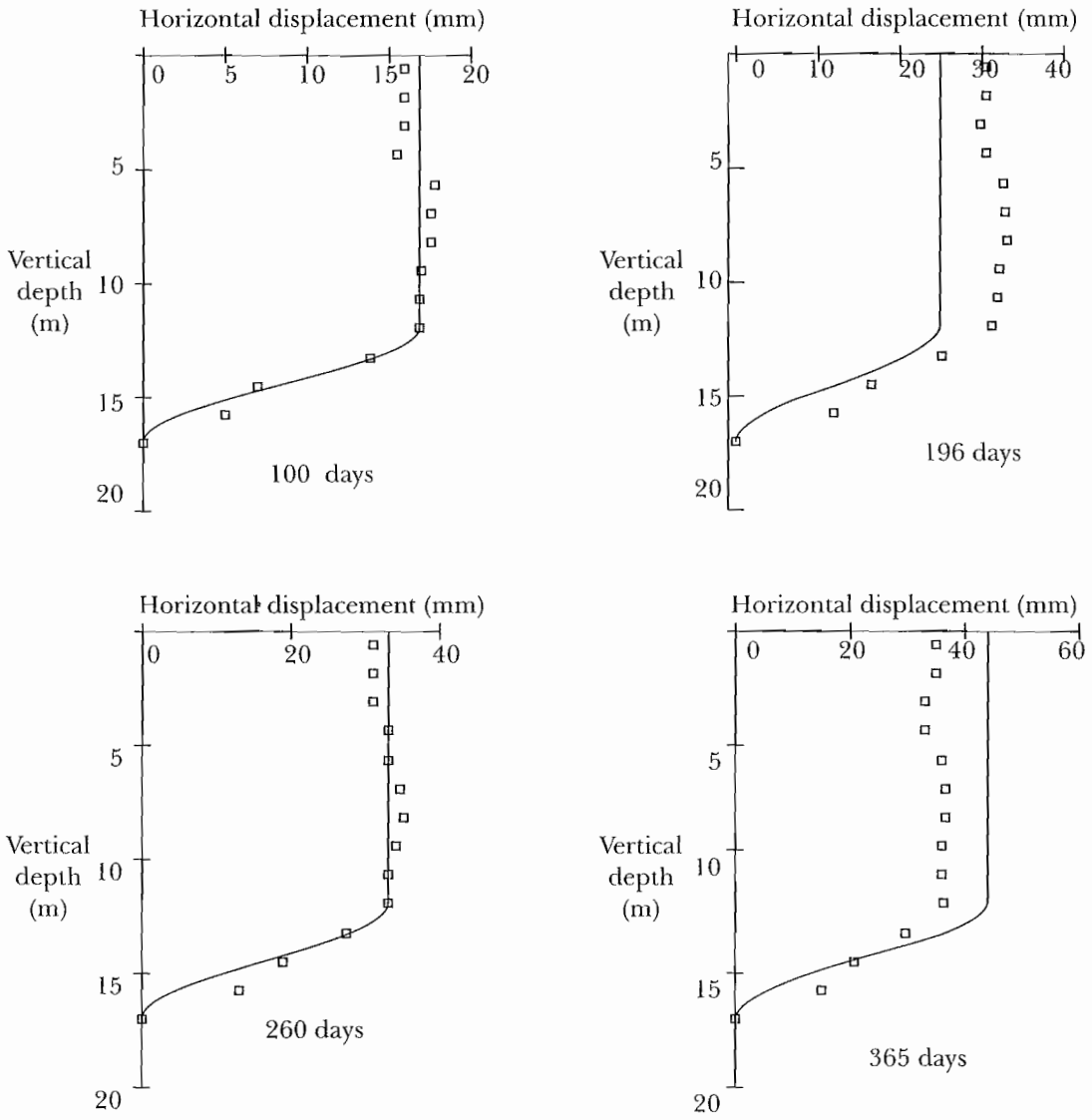

Fig. 7 – Villaberney landslide. Experimental displacement profiles (symbols) and model predictions (solid line) at location E_1 after a period of 100, 196, 260, and 356 days.

Fig. 7 - Frana di Villaberney. Profili di spostamento misurati (simboli) e previsioni del modello (linea continua) in E_1 dopo un periodo di 100, 196, 260 e 356 giorni.

$$\eta = \Delta t \left[\frac{\frac{\alpha}{6}(y_B - y_T)^3 \tan\theta + \frac{\gamma_0 \sin\theta}{2}(y_B - y_T)^2}{u(y_T)} + \frac{-k_0 (y_B - y_T) - \frac{\beta}{y_0^n}\frac{(y_B^{n+1} - y_B^n)}{n+1}}{u(y_T)} \right] \quad (23)$$

with $u(y_T)$ the measured displacement of the top layer.

4. Field behaviour predictions

In this section, the model proposed is used to describe the movements of two natural slopes (a) Villarbeney, Switzerland [data reported in DESAI *et al.*, 1995] and (b) Fosso San Martino, Italy [data after BERTINI *et al.*, 1984].

Villaberney landslide

The model is used to backpredict observed field behaviour over one year time interval at two locations, E_1 and E_2. Piezometric readings indicate that the ground-water level didn't vary significantly in the time period considered. No significant movements were observed at depths beyond 17 m for location E_1, and 7.5 m for location E_2. The base slope angle at location E_1 is $\theta = 14°$, while at E_2 it is $\theta = 17°$. The reported pattern of displacements is shown in Fig. 5. At location E_1, the upper limit of the shear

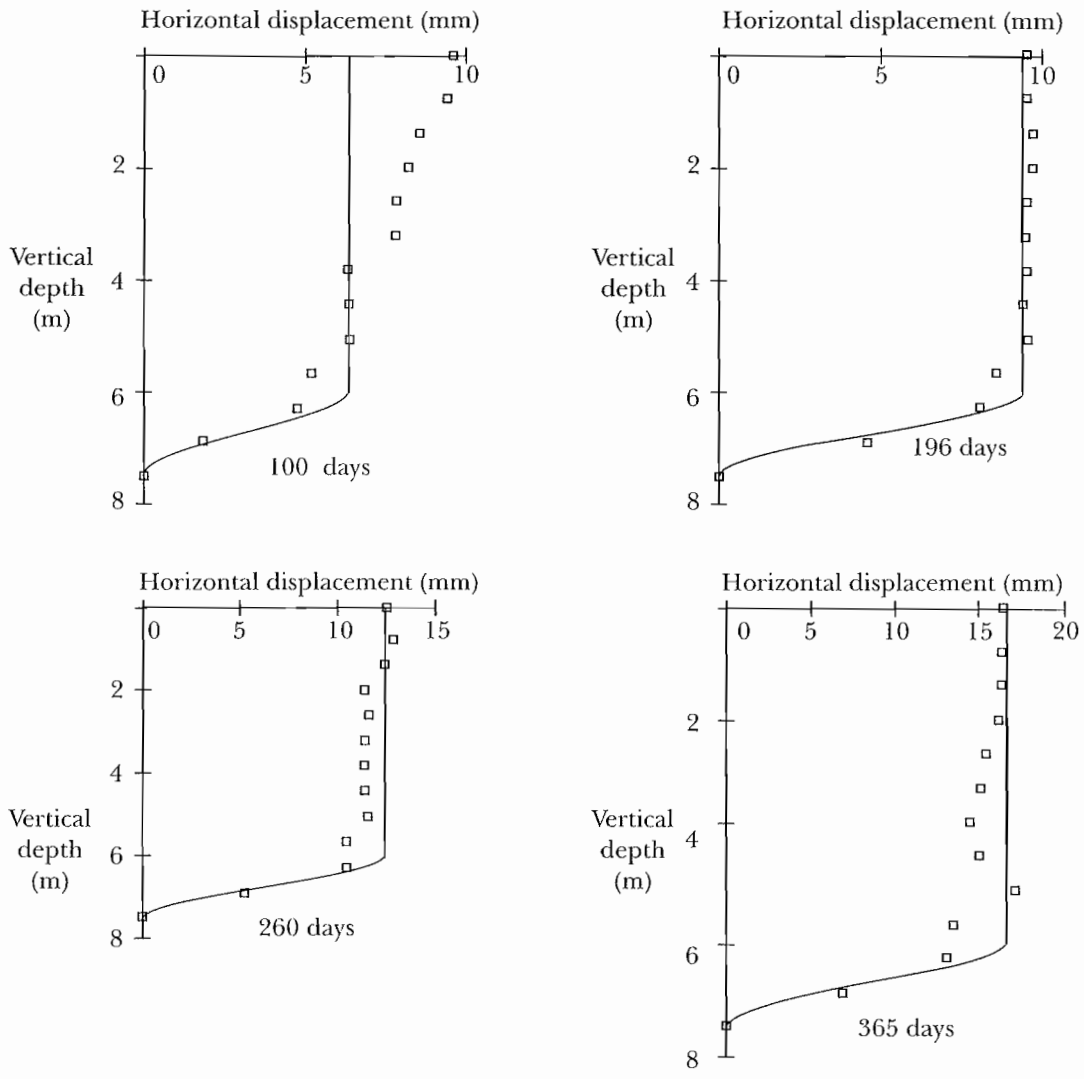

Fig. 8 – Villaberney landslide. Comparison between theoretical (solid line) and experimental (symbols) displacement profiles at location E_2 after a period of 100, 196, 260, and 356 days.
Fig. 8 - Frana di Villaberney. Confronto fra i profili di spostamento teorici (linea continua) e misurati (simboli) in E_2 dopo un periodo di 100, 196, 260 e 356 giorni.

zone is $y_T = 11.6\ m$ and the lower limit is $y_B = 17.5\ m$, while at location E_2: $y_T = 5.74\ m$ and $y_B = 7.65\ m$. The reported values for the unit weight γ_0 at the surface are: 21.8 kN/m^3 (location E_1) and 21.6 kN/m^3, respectively; the values of α in Eq. (4) are $\alpha = 0.024$ kN/m^4 (location E_1) and 0.089 kN/m^4 at location E_2 [see DESAI *et al.*, 1995]. The greater value of the coefficient α at E_2 location indicates that the creeping mass near E_2 is older and more consolidated than near E_1 We take $y_0 = 1\ m$ and assume $k_0 = 10$ kPa, the estimate of the yield limit at the ground surface being based on the value of cohesion for silty sand (see [TERZAGHI, *et al.*,1996]. Using the procedure presented in the previous section [see Eqn. (22)] we

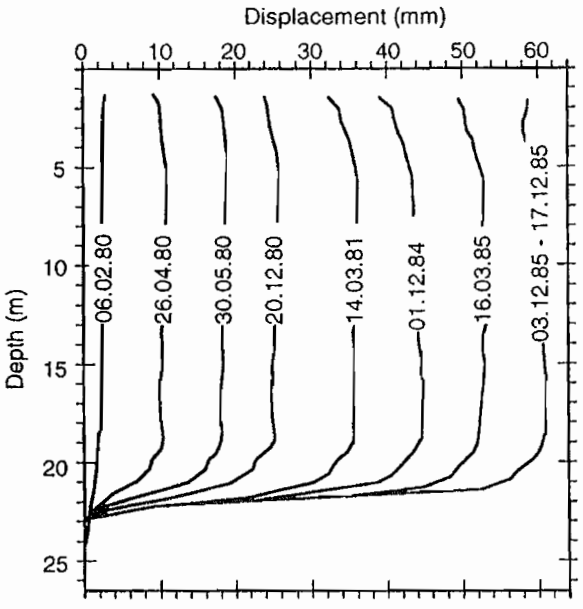

Fig. 9 – Fosso San Martino. Inclinometers readings [after BERTINI *et al.*, 1984].
Fig. 9 – Fosso San Martino. Letture inclinometriche [da BERTINI et al. 1984].

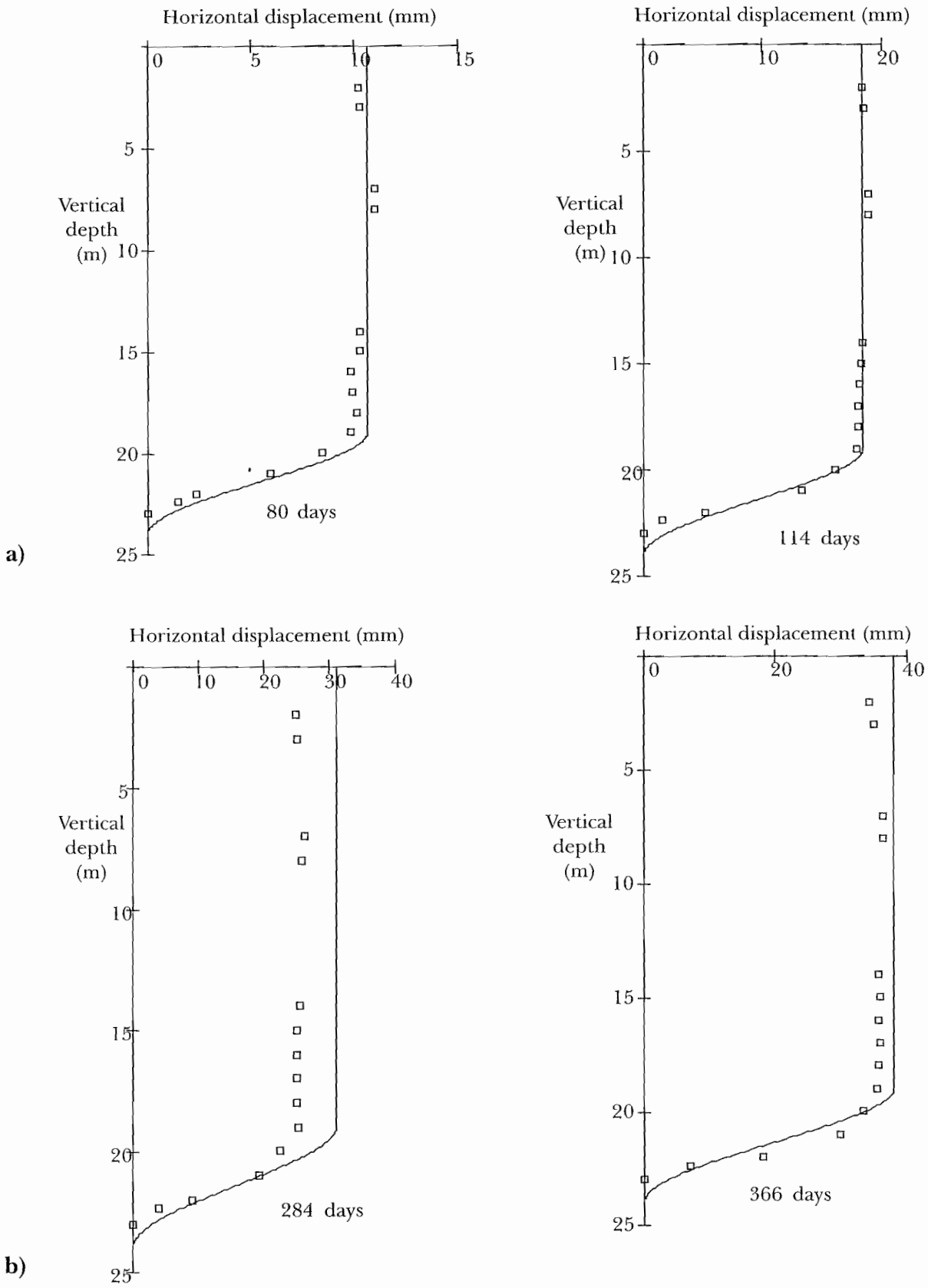

Fig. 10 - Fosso San Martino Landslide. Theorethical predictions (solid lines) and experimental (symbols) displacement profiles for the time intervals: (a) 80 and 114 days; (b) 284, and 366 days.

Fig. 10 – Fosso San Martino. Profili di spostamento teorici (linea continua) e misurati (simboli) per gli intervalli di tempo: (a) 80 e 114 giorni; (b) 284 e 366 giorni.

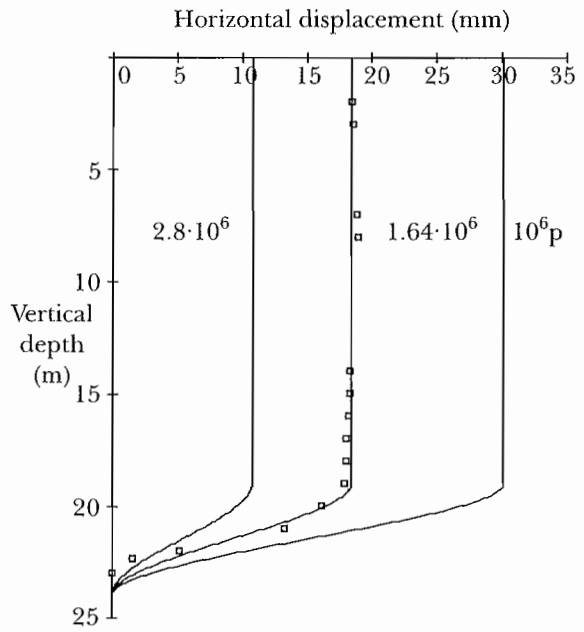

Fig. 11 – Influence of the viscosity on the creep flow. Experimental data (symbols) from Fosso San Martino [reported in BERTINI *et al.* 1984] correspond to displacements registered between February 6, 80 and April 4, 80.
Fig. 11 – Influenza della viscosità sugli scorrimenti lenti. Dati sperimentali (simboli) da Fosso San Martino [riportati in BERTINI et al. *1994] corrispondenti agli spostamenti registrati tra il 6 febbraio 1980 ed il 4 aprile 1980.*

obtain: $n = 1.17$ and $\beta = 3$ kPa at location E_1 and $n = 1.33$ and $\beta = 2.62$ at location E_2. As an example, in Fig. 6 are shown the variation of the shear stress $T_{xy}(y)$ and of the yield limit $k(y)$ with depth at location E_1. For that value of n, $T_{xy}(y) = k(y)$ at y_T and y_B and $k(y)$ is nearly tangent to $T_{xy}(y)$ all along the interval $y_T < y < y_B$ (the slope of $k(y)$ is very close to that of $T_{xy}(y)$); in the interval $y_T < y < y_B$: $|Txy(y)| > k(y)$. Hence, creep flow initiates in an entire zone and sliding is not restricted to a thin layer (sliding discontinuity surface).

Based on the inclinometers readings at November 9, 78 and April 5, 79 ($\Delta t = 148$ days) in conjunction with (23) we get a viscosity coefficient $\eta = 2.84\times10^6 P$ at location E_1. Using the measurements over 196 days (November 9, 78 and May 25, 79) we calibrate $\eta = 5.02\times10^5 P$ at location E_2. Figures 7 and 8 shows the theoretical displacement profiles (obtained using (28)) after a period Δt of 100, 196, 260, and 356 days together with the field data at locations E_1 and E_2, respectively. The model compares very well with the observed displacement profiles.

Fosso San Martino landslide

The model was also used to predict landslide activities in a slope of Fosso San Martino basin. The field data were reported in [BERTINI *et al.* 1984; 1986]. The movements involve a detrital cover reaching 20-25 m in thickness and a softened part of the marly clay bedrock. The slides are characterized by a very low displacement rate (1-2 cm/year) on average. The movements strongly depend on the rainfall amount and regime. Depending on location in the landslide body, inclinometers indicate either rigid or viscous displacement profiles (see Fig. 9). The shear zone is located in the softened bedrock, its upper limit being at $y_T = 17.8m$, while its lower limit is $y_B = 21.6\ m$. Above the shear zone a rigid body motion is observed; no movements are registered below a depth of 22.5 m. The slope base angle is $\theta = 20°$. No data concerning the unit weight were reported. For this reason, we have assumed that the unit weight γ_0 at the surface is 10 kN/m^3 based on the values of the values of unit weight in dry state for soft clay [see TERZAGHI *et al.*, 1996]; the values retained for the coefficient α of Eq. (4) are: $\alpha = 0.15$ kN/m^4 (April), $\alpha = 0.06$ kN/m^4 (May), $\alpha = 0.24$ kN/m^4 (December) and 0.26 kN/m^4 (March). We take $y_0 = 1\ m$ and assume $k_0 = 14$ kPa, this estimate of the yield limit being based on the value of cohesion for soft clay [see TERZAGHI, *et al.*,1996]. From (22) we obtain: $n = 1.38$, 1.31, 1.44, and 1.45, respectively while $\beta = 1.03$, 1.14, 0.96, and 0.95, respectively. Based on the inclinometers readings on February 6, 80 and May 30, 80 ($\Delta t = 114$ days) we have found a viscosity coefficient of $\eta = 1.64\times10^6 P$. Figures 10a and 10b show the theoretical displacement profiles after a period of 80, 114, 284, and 366 days(February 6,80 till March 14, 81) together with the field data. The model reproduces the main features of the observed behaviour. The influence of the value of η, when the other parameters are fixed can be clearly seen in Figure 11 (experimental points correspond to time interval of Δt of 114 days.

5. Conclusion

A model for describing landslides was proposed. The geological material was modeled as a non-homogeneous Bingham fluid. This constitutive equation allows for a variation of density and yield stress with depth. A criterion for shear flow initiation is formulated and the ensuing motion is described. Generally, at a certain depth there is a shear region, the top layer above is in rigid motion (unless the cohesion is zero) while the layer below the shear region is rigid and at rest. A procedure for determination the constitutive parameters of the model based solely on field observations of natural slopes was outlined. The model is used to predict the observed field behaviour at two sites, one in Switzerland and the other in Italy. Compar-

ison between the theoretical predictions and measured displacement profiles are reasonably good, with accuracy within the experimental scatter.

References

ANCEY C., COUSSOT P. and EVESQUE P. (1996) – *Examination of the possibility of a fluid- mechanics treatment of dense granular flows*. Mechanics of Cohesive-Frictional Materials. vol. I, n. 4, pp. 385-403.

BERTINI T., CUGUSI F., D'ELIA B. and ROSSI-DORIA M. (1984) – *Climatic conditions and slow movements of colluvnal covers in Central Italy*. Proc. IV Int. Symp. on Landslides, Toronto, vol. I, pp. 367-376.

BERTINI T., CUGUSI F., D'ELIA B. and ROSSI-DORIA M. (1986) – *Lenti movimenti di versatile nell'Abruzzo adriatico: caratteri e criteri di stabilizzazione*. Proc. XVI Conv. Naz. Di Geotecnica, Bologna, vol. I, pp. 91-100.

BRUNSDEN D. (1984) – *Mudslides*. in Slope Instability, John Wiley & Sons, Chichester, pp. 363-418.

CRISTESCU N. (1989) – *Rock Rheology*. Kluwer Academic, Dordrecht.

CRISTESCU N.D., CAZACU O. and CRISTESCU C. (1998) – *Compaction and gravitational creep flow of granular meterials*. Proc. 35th Annual Technical Meeting of Society of Engineering Science, Pullman, Washington, pp. 70.

CRISTESCU N.D., CAZACU O. and CRISTESCU C. (2000) – *A model for landslide*. (submitted to Can. Geotech. J.).

DESAI C.S., SAMTANI n. C. and VULLIET L. (1995) – *Constitutive Modeling and Analysis of Creeping Slopes*. J. of Geotechnical Engineering, *ASCE*, vol. CXXI, n. 1, January, pp. 43-56.

D'ELIA B., PICARELLI L., LEROUEIL S. and VAUNAT J. (1998) – *Geotechnical characterization of slope movements in structurally complex clay soils and stiff jointed clays*. Rivista Italiana di Geotecnica, vol. XXXII, n. 3, pp. 5-29.

HUTTER, K. (1993) – *Continuum description of natural slopes in slow movement*. In CISM Courses and Lectures, n. 337, Springer-Verlag, Wien-New York, pp. 241-311.

LIU K.F. and MEI C.G (1989) – *Slow Spreading of a Sheet of Bingham fluid on an Inclined Plane*. Journal of Fluid Mechanics, vol. CCVII, pp. 505-529.

PERZYNA P. (1966) – *Fundamental Problems in Viscoplasticity*. Adv. in Appl. Mech., vol. IX, pp. 243-377.

SAMTANI n. C., DESAI C.S. and VULLIET L. (1996) – *An Interface Model to describe Viscoplastic Behavior*. Int. J. for Num. and Analyt. Meth. in Geomechanics, vol. XX, n. 4. pp. 231-252.

SAVAGE S.B. and HUTTER K. (1991) – *The dynamics of avalanches of granular materials from initiation to runout. Part I: Analysis*. Acta Mech (1-4), vol. LXXXVI, pp. 201-223.

SOUSA J. and VOIGHT B. (1991) – *Continuum simulation of flow failures*. Géotechnique, vol. XLI, pp. 515-538.

TERZAGHI K., PECK R.B., and MESRI G. (1996) – *Soil Mechanics In Engineering Practice*. 3rd ed., John Wiley & Sons, New York, Chichester, Brisbane, Toronto, Singapore.

TER-STEPANIAN G. (1973) – *New rheological model of creep of a clay at shear*. Reported at the Symposium on the Theory of Landslide Processes, May, Dilijan.

VULLIET L. and HUTTER K. (1988 a) – *Set of constitutive models for soils under slow movement*. J. of Geot. Eng. Div., *ASCE*, vol. CXIV, n. 9, pp. 1022-1041.

VULLIET L. and HUTTER K. (1988 b) – *Continuum model for natural slopes in slow movement*. Géotechnique, vol. XXXVIII., n. 2, pp 199-217.

VULLIET L. (1988c) – *Viscous-type sliding laws for landslides*. Can. Geotech. J., n. 25, pp. 467-477.

Modello costitutivo ed analisi di movimenti lenti di pendii naturali

Sommario

Si propone un nuovo modello per la descrizione dei movimenti lenti di pendio. Il materiale geologico del pendio è modellato mediante un'equazione costitutiva non omogenea di Bingham. Questo modello considera l'effetto della consolidazione gravitazionale sulla risposta del materiale e quindi della variazione della tensione di plasticizzazione e di densità con la profondità. Si formula un criterio per l'inizio del movimento e se ne descrive il flusso seguente. Si presenta una procedura diretta per la determinazione dei parametri del modello basata unicamente sui dati ricavati da prove in sito. Per illustrare questa procedura e l'idoneità e potenzialità del metodo proposto, i dati riportati in letteratura sono stati usati per predire il comportamento (andamento degli spostamenti misurati) di due colate verificatesi in Svizzera ed Italia. Il confronto fra le previsioni teoriche ed i profili di spostamento misurati è ragionevolmente buono, considerata la dispersione dei dati sperimentali.